Journal of Applied Polymer Science

Morphology modulation of gas-foamed, micrometric, hollow polystyrene particles

Vincenzo Contaldi,[1,2] Luigi Imperato,[1] Silvia Orsi,[3] Ernesto Di Maio,[1] Paolo Antonio Netti,[1,3] Salvatore Iannace[4]

[1]Dipartimento di Ingegneria Chimica dei Materiali e della Produzione Industriale, University of Naples Federico II, Piazzale Tecchio 80, Naples 80125, Italy

[2]Technological District, CRdC Tecnologie Scarl, Via Nuova Agnano 11, Naples 80125, Italy

[3]Center for Advanced Biomaterials for Health Care, Istituto Italiano di Tecnologia, Largo Barsanti e Matteucci 50, Naples 80125, Italy

[4]Istituto per lo Studio delle Macromolecole, Consiglio Nazionale delle Ricerche, Via Edoardo Bassini 15, Milan 20133, Italy

Correspondence to: E. Di Maio (E-mail: edimaio@unina.it)

ABSTRACT: In this article, we reports the effects of the processing conditions on the morphological and hollow attributes of polystyrene micrometric hollow particles produced by the use of a recently developed technique based on the gas foaming of spherical, dense particles. By modulating the foaming temperature and saturation pressure, we produced hollow particles with different attributes in terms of hollow dimensions, eccentricity, and open–close features. The results from these small systems were compared, and we found agreement with what is typically observed in bulk polymeric foaming, for example, an increase in the foaming efficiency with saturation pressure and the nonmonotonic effect of temperature. Furthermore, we observed an increase in the hollow number when using nucleating agents with respect to the neat polymer and when using nitrogen with respect to carbon dioxide as the blowing agent. The effects of particle manipulation before foaming to achieve hollow elongated or distorted particles are also reported. © 2016 Wiley Periodicals, Inc. J. Appl. Polym. Sci. **2016**, *133*, 44236.

KEYWORDS: asymmetry; hollow; gas foaming; microparticle

Received 27 March 2016; accepted 27 July 2016

DOI: 10.1002/app.44236

INTRODUCTION

Hollow nanoparticles and microparticles are gaining technological and scientific importance in a growing number of applications, including catalysis, cosmetics, drug and gene delivery, diagnostics, and pollutant removal. In drug and gene delivery, for example, the hollow particle has been successfully filled with drugs and DNA for target release in a controlled manner.[1] In other areas, the void space has been used to modulate the refractive index of the particle or to focus lasers.[2] Hollow particles are typically prepared by emulsion polymerization, suspension polymerization, core–shell precursors, self-assembly, spraying, electrospraying, template-directed synthesis, and microfluidics.[3,4] These methods have been used extensively to produce hollow particles of many different sizes with many polymers. As a matter of fact, most of the reported particles have had a spherical shape. The achievement of nonspherical particles, conversely, has been reported to be a critical need, for instance, in biomedicine and pharmacology[5] and chemistry.[6]

In the past 3 decades, the foaming behavior of a great number of polymers [e.g., particularly polypropylene,[7–11] polystyrene (PS),[12–15] and polycarbonate[16–18]] with environmentally benign gases, such as carbon dioxide (CO_2) or nitrogen, has been studied extensively. Detailed analyses of the foaming process in terms of the effects of the processing parameters on the final foam structure have been conducted. As a general understanding, the main process parameters are the temperature at which thermodynamic-instability-promoting bubble nucleation is induced (foaming temperature) and the saturation pressure. In particular, it has been observed that increases in the foaming temperature and saturation pressure both induce an increase in the bubble size. Furthermore, an increase in the foaming temperature reduces the viscosity of the material and, above certain

Additional Supporting Information may be found in the online version of this article.

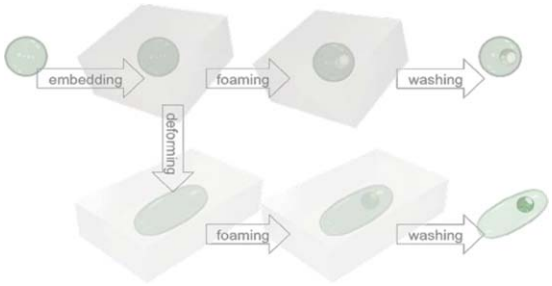

Figure 1. Schematic illustration of the preparation of the foamed, hollow particles. [Color figure can be viewed at wileyonlinelibrary.com.]

ranges, typically induces a weakening of the polymer; this induces cell coalescence and foam collapse.

We recently introduced a gas-foaming technique to produce hollows in dense microparticles and nanoparticles made of PS and of poly(lactic-*co*-glycolic acid).[4] As illustrated in the scheme in Figure 1, the key was to embed the dense particles into a barrier film made of water-soluble poly(vinyl alcohol) (PVA) before saturation with a foaming gas such as CO_2 at high pressures. After a sudden release of the saturating pressure, the previously solubilized gas nucleated and grew to blow the particles. The impermeable barrier film prevented the foaming gas from diffusing out of the particles before foaming. The particles with hollows could be obtained after water washing to remove the barrier film. An advantage of this method was that the films with embedded particles could be stretched one-dimensionally or two-dimensionally to deform the embedded particles before gas foaming. Thus, various nonspherical particles with hollows could be produced. However, no detailed study on the morphology modulation of the foamed particles was performed in the previous work.

In this study, we used the gas-foaming method to foam PS particles with a diameter of 5 μm and studied the effects of the processing conditions in a wide range of foaming temperatures and saturation pressures. To show the full potential of the technique, we further report the effects of the use of mixtures of blowing agents and nucleating agents on the morphology of the resulting hollow particles. These effects were compared to dependences typically observed on bulk polymer foaming.

EXPERIMENTAL

The method used to foam PS particles has been reported in ref. 4 and makes use of a barrier film made of PVA to contain and hinder the blowing agent from escaping from the particle. Figure 1 schematizes the whole processing stage, which consists of the embedding of the bare, dense, spherical particle in a film of a water-soluble polymer with barrier properties toward the blowing agent to be used in foaming. Before foaming, it was possible to manipulate the film embedding into the particles to change their shape, to confer, for example, an ellipsoidal shape, as in the example depicted in Figure 1.[4] In more detail, the barrier-film-embedded PS spheres were prepared as follows: 0.1% w/v uncrosslinked PS spherical particles (5 μm in diameter, Duke Scientific) were dispersed in aqueous solutions of 5% w/v PVA (molecular weight ≈ 205 kg/mol, Mowiol 40-88, Sigma-Aldrich) and 2% w/v of glycerol. The obtained mixtures were carefully poured into Teflon molds with flat surfaces and left to dry at room temperature for 72 h.

For the production of foamed samples, a thermoregulated pressure vessel having a volume of 0.3 L (model BC-1, HiP, Erie, PA) was used. The pressure discharge system consisted of a discharge valve (model 15-71 NFB, HiP), an electromechanical actuator (model 15-72 NFB TSR8, HiP), and an electrovalve.

The pressure history was registered with a data acquisition system (DAQ PCI6036E, National Instruments) and a pressure transducer (model P943, Schaevitz-Measurement Specialties, Hampton, VA). In a typical experiment, the samples (barrier-film-embedded PS spheres) were loaded into the vessel, pressurized with the blowing agent mixture at a saturation pressure ranging from 6.0 to 18.0 MPa at 60–130 °C for 2 h, and finally, pressure-quenched at 100 MPa/s at a foaming temperature equal to the saturation temperature. Particles were recovered by the dissolution of the PVA films in water at room temperature and washed by centrifugation with water five times. Each of the reported foaming conditions was used in three replicates. To investigate the effect of the nucleating agents, magnetic uncrosslinked PS spherical particles (Bangs Laboratories, Inc.)[19] were used. In fact, these micrometric particles contained iron oxide nanometric particles and are used for, among other things, diagnostics. In our case, we were only interested in the presence of the inorganic filler, which could serve as a bubble nucleating agent.[4] To verify the particle morphology by scanning electron microscopy (SEM), the foamed particles were coated with gold (Cressington 208HR, high-resolution sputter coater) and imaged with a field emission gun scanning electron microscope (Carl Zeiss Ultra Plus). To evaluate the efficiency of the foaming method, optical microscopy (Olympus IX81) was used to count the particles with and without bubbles. The fraction of foamed particles was calculated on the basis of about 50 individual particles. The particles were large and transparent enough to identify hollows in individual particles (see Supporting Information, Figure S1). In the design of hollow particles for a specific application, a key feature is represented by the open–closed nature of the porosity because it establishes, for example, the possibility of accessing the hollow for subsequent filling. The possibility of modulating this hollow feature and the pore dimensions and number, through changes in the process conditions, was assessed by the variation of the processing conditions, the blowing agent mixture, and the use of nucleating agents, as follows.

RESULTS AND DISCUSSION

Effect of the Saturating Pressure

Figure 2 shows selected SEM images of the 5 μm PS particles foamed at 100 °C after saturation at a pressure of CO_2 ranging from 6.0 to 18.0 MPa. The results of the morphological analysis by SEM and optical microscopy are reported in Figure 3.

As shown in Figure 2, at low saturation pressures (6.0 and 8.0 MPa), few particles were effectively foamed, and because of the small amount of solubilized gas, closed pores were rarely achieved. At higher pressures (from 10.0 MPa), as expected, there was a

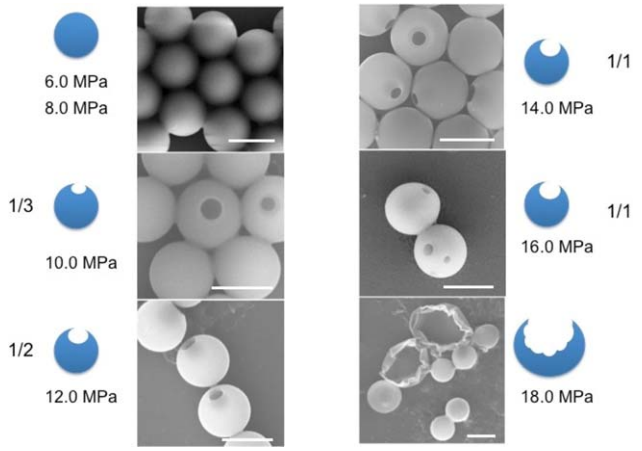

Figure 2. Effect of the CO_2 pressure on the morphology of 5 μm foamed PS particles (foaming and saturation temperature = 100 °C). The scale bars represent 5 μm. The saturation pressure is reported next to the corresponding micrograph together with the fraction of particles containing a hole and with a schematic of the morphology of the resulting foamed particle. [Color figure can be viewed at wileyonlinelibrary.com.]

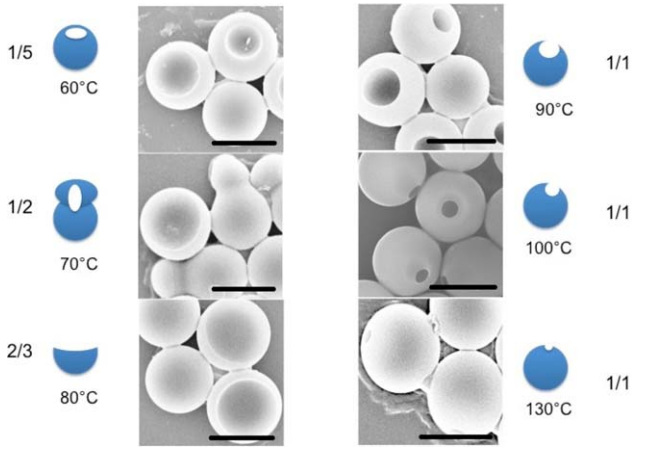

Figure 4. Effect of the saturation and foaming temperatures on the morphology of the 5 μm foamed PS particles (saturation CO_2 pressure = 14.0 MPa). The scale bars represent 5 μm. The saturation and foaming temperatures are reported next to the corresponding micrograph together with the fraction of particles containing a hole and with a schematic of the morphology of the resulting foamed particles. [Color figure can be viewed at wileyonlinelibrary.com.]

strong effect of the saturation pressure on the particle morphology because of the increased amount of gas solubilized into the polymer. It is well known, in fact, that in the case of bulk polymers, the saturation pressure extensively affects both the foam density and the morphology. Namely, the increase of the gas saturation pressure typically induces an increased volume expansion (more gas is available for inflating the newly formed bubbles) and a corresponding decrease in the final foam density. When the gas solubilized in the polymer is above a certain limit (which depends on a multitude of properties of the polymer–blowing agent couple, e.g., the melt strength of the polymer and the polymer–gas mutual diffusivity), the polymer may not be able to withstand the elongational stresses exerted during bubble growth and may rupture. This occurrence sets the foamability limit of the polymer–gas solution under investigation. In our case, we drew the particle diameter versus saturation pressure to demonstrate the degree to which the particles were inflated. Figure 3 shows the effect of the saturating pressure on both the foamed particle diameter and the hollow opening diameter at foaming temperatures of 80 and 100 °C. As was possible to observe, the increase in the saturation pressure determined the increase in the foam efficiency until the collapse of the particle (at a saturation pressure of 18.0 MPa), where, in particular in the case of a foaming temperature of 100 °C, the particles appeared completely deformed and burst (see also Figure 2) for the extreme foaming conditions and the lower polymer viscosity and melt strength at high temperature. This occurrence may be considered analogous to the foam collapse and densification. At the two different temperatures, the effect of the saturation pressure on the hollow opening diameter was different. At 80 °C, it attained a maximum at 12.0 MPa, where the opening diameter reached approximately 2 μm, whereas at 100 °C, it was almost constant up to a pressure of 18.0 MPa, where, as we mentioned, the particles burst, and the opening reached an external particle diameter of approximately 5 μm.

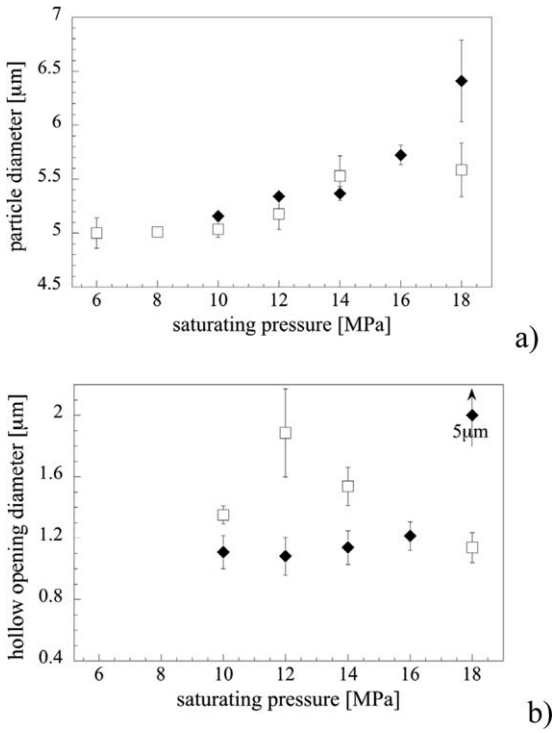

Figure 3. Effect of the CO_2 pressure at different foaming temperatures on the (a) final particle diameter and (b) hollow opening diameter. Open symbols indicate a foaming temperature of 80 °C, and closed symbols indicate a foaming temperature of 100 °C.

Effect of the Foaming Temperature

Figure 4 shows selected SEM images of the 5 μm PS particles saturated with CO_2 at a pressure of 14.0 MPa and a saturation and foaming temperature ranging from 60 to 140 °C (direct gas release at the end of sorption, without temperature change). The results of the morphological analysis by SEM and optical

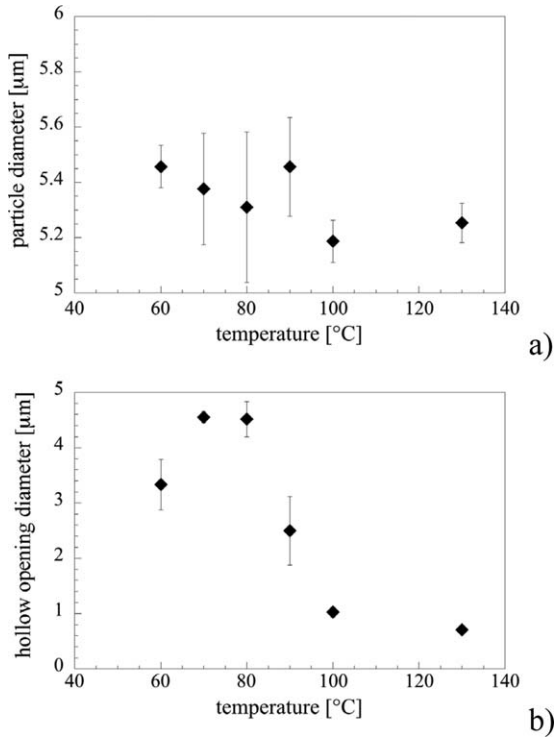

Figure 5. Effect of the foaming temperature on the (a) final particle diameter of the 5 µm foamed PS particles and (b) hollow opening diameter (after saturation with CO_2 at 14.0 MPa).

microscopy are reported in Figure 5. As is well known, the increase of the saturation temperature determined the reduction of the CO_2 concentration in the PS–CO_2 solution, as reported, for instance, by Sato *et al.*[20] Hence, with increasing saturation (and foaming) temperature, the polymer softened, but with a lower amount of solubilized CO_2, the plasticization effect by CO_2 was reduced. This partially compensated for the temperature increase. More importantly, the blowing agent availability was reduced. As a result of these counteracting effects, the foaming temperature had a minor effect on the particle diameter and showed a nonsignificant difference ($p = 0.314$), as depicted in Figure 5(a). Conversely, the pore opening diameter increased up to temperatures of 70–80 °C and decreased at temperatures higher than 80 °C ($p = 0.004$), as depicted in Figure 5(b).

Effect of the Blowing Agent Composition

The blowing agent, of course, played a major role in gas foaming, as has been reported in the literature for several polymer–blowing agent systems. Typically, for instance, CO_2 has a good solubility in polymers and, correspondingly, may generate high volume expansions. N_2, conversely, typically has a lower solubility and gives foams with a low volume expansion (higher density foams). As a counterpart, however, foams blown with N_2 are typically characterized by a finer morphology with respect to CO_2 as a result of their higher diffusivities. When a compromise between low densities and fine morphologies is to be reached, a N_2–CO_2 mixture can be used.[21] In our case, in exploring the effect of the blowing agent composition, we also observed the same effect. Of course, with such small particles, as was the case in this study, we just achieved one or few pores. This effect was

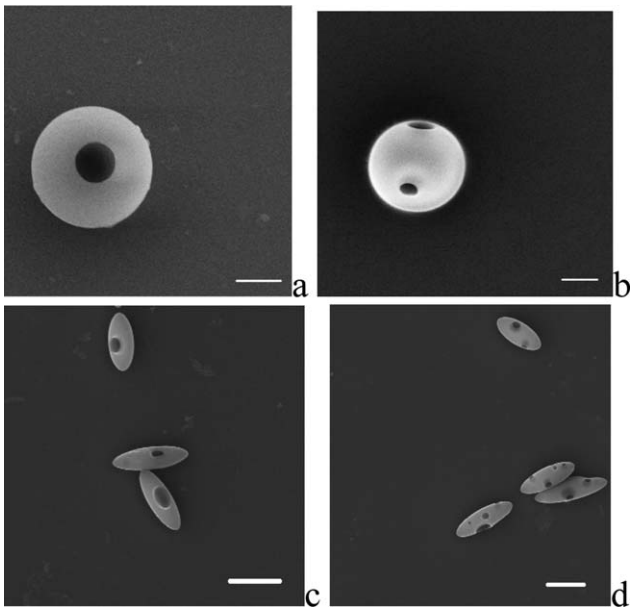

Figure 6. Effect of the blowing agent composition on the morphology of the foamed, micrometric particles: spherical particles foamed (a) at 100 °C after CO_2 saturation at 16.0 MPa and (b) at 100 °C after saturation with an 80–20 vol % N_2–CO_2 mixture at 16.0 MPa and ellipsoidal particles foamed (c) at 100 °C after CO_2 saturation at 16.0 MPa and (d) at 100 °C after saturation with an 80–20 vol % N_2–CO_2 mixture at 18.0 MPa.

first reported in our previous work on spherical particles.[4] Here, we included the effect of the blowing agent composition on ellipsoidal particles. Figure 6 reports the effect of the blowing agent composition on particle foaming with CO_2 and an 80/20 vol % N_2–CO_2 mixture on spherical and ellipsoidal particles; this shows the greater nucleation efficiency of N_2 with respect to CO_2 (which was, conversely, responsible for the bigger pores). This effect has been extensively reported in the foaming literature of bulk polymers[21,22] and was in agreement with our results on such small particles.[4]

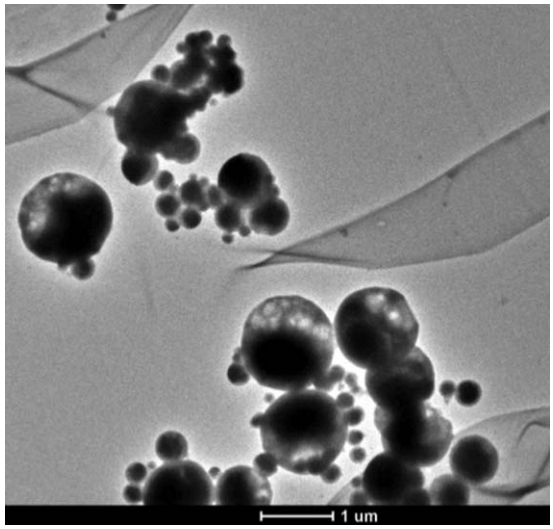

Figure 7. Effect of nucleating agents on 1-µm PS particles containing iron oxide that foamed at 100 °C after CO_2 saturation at 14.0 MPa.

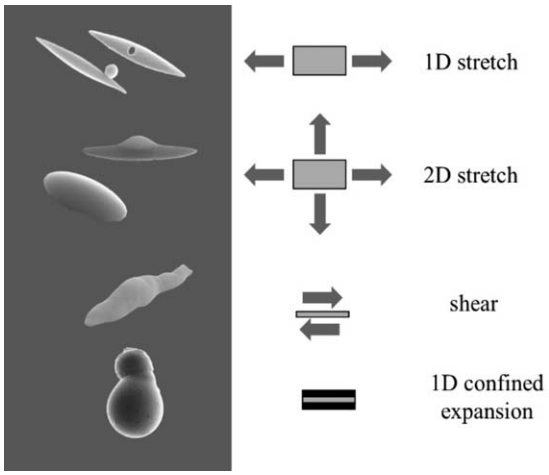

Figure 8. Effect of particle manipulation before foaming on the morphologies of the final hollow particles.

Effect of the Nucleating Agents

Nucleating agents are frequently used in polymeric foaming to control the porous morphology and to induce more bubbles with respect to formulations without nucleating agents. Heterogeneous versus homogeneous nucleation is the involved mechanism. To verify the effect of the nucleating agents in the foaming of micrometric particles, we used PS particles containing iron oxide; these particles are used for their magnetic properties in biological applications.[19] Figure 7 shows an SEM image of the foamed 1-μm PS particles containing iron oxide nanometric particles, which in this context, acted as nucleating agents for CO_2 bubbles (cf. Figures 2 and 4).

Effect of the Particle Pretreatment

With respect to the technologies available to produce hollow particles listed in the Introduction, the introduction of the gas-foaming method to produce hollow micrometric and nanometric particles represents a breakthrough in the framework of microparticles and nanoparticles. The method, in fact, is characterized by great versatility in terms of particle size, material, and hollow features, and more importantly, it separates the particle-formation stage from the hollow-formation stage. In emulsion polymerization, for instance, the hollow particle is achieved by a controlled polymerization of the monomer sitting at the water–oil interface of the drop in a single step. In our case, dense particles of any diameter, size, or material were postprocessed to achieve the hollow.[4] This, apart from the tremendously ease of the involved chemistry to produce the particles, gave us the opportunity to manipulate the particles, for example, through stretching and shearing, before foaming to achieve nonspherical shapes.[4] For example, elongation in one direction, as was introduced by Champion and Mitragotri,[23] gives ellipsoidal particles, which can be subsequently foamed to achieve hollow elongated particles that resemble microkayaks and nanokayaks, as reported in our previous article.[4] The imaginative use of this opportunity gave us the chance to produce a lot more shapes of nonspherical hollow particles, as reported in Figure 8. Hollow microkayak, unidentified flying object (micro-UFO), microworm, and microsnowman-like particles were achieved through the gas foaming of one-dimensional (1D) elongated, two-dimensional (2D) elongated, sheared, and confined particles, respectively.

As shown previously, with this study, we gained a comprehensive view on the use of the foaming technique to produce hollow polymeric particles of desired shapes and hollow features. The robustness of the gathered results allowed us to seek to exploit the properties of these systems. For instances, particles with open porosities, such as those achieved at 100 °C and 14.0 MPa, were recently filled with gadolinium, which is used as a contrast agent, and subsequently closed by a swelling agent[24] to produce easy-to-fill asymmetric polymeric microreservoirs with potential application for diagnostics.[25] An experimental campaign is ongoing on the filling and closing of these particles with quantum nanodots for electronic applications. Finally, bare, hollow 500-nm particles are under investigation under visible-light wavelengths for possible use in optics.

CONCLUSIONS

The effects of the processing conditions and other strategies for modifying foam densities and morphologies were adopted in this study to achieve foamed hollow PS micrometric particles with several morphological features. The effects observed in the underlying literature on bulk polymeric foaming were also observed in such small systems. Open and closed porosities and several dimensions and shapes were achieved in temperature and pressure ranges from 60 to 130 °C and 6.0 to 18.0 MPa, respectively. Finally, we achieved nonspherical hollow particles by taking advantage of the separation between the particle-formation step and the hollow-formation step.

ACKNOWLEDGMENTS

Rete di Eccellenze Mastri (Materiali e Strutture Intelligenti, POR Campania FSE 2007/2013, Codice 4-17-3) is acknowledged for partial funding of this work. The authors thank Manlio Colella for the scanning electron microscopy (SEM) observations.

REFERENCES

1. De Koker, S.; De Cock, L. J.; Rivera-Gil, P.; Parak, W. J.; Velty, R. A.; Vervaet, C.; Remon, J. P.; Grooten, J.; De Geest, B. G. *Adv. Drug Delivery Rev.* **2011**, *63*, 748.
2. Li, X.; Gao, J.; Xue, L.; Han, Y. *Adv. Funct. Mater.* **2010**, *20*, 259.
3. Wang, A. J.; Lu, Y. P.; Sun, R. X. *Mater. Sci. Eng.* **2007**, *460*, 1.
4. Orsi, S.; Di Maio, E.; Iannace, S.; Netti, P. A. *Nano Res.* **2014**, *7*, 1018.
5. Decuzzi, P.; Pasqualini, R.; Arap, W.; Ferrari, M. *Pharm. Res.* **2009**, *26*, 235.
6. Xing, S. X.; Feng, Y. H.; Tay, Y. Y.; Chen, T.; Xu, J.; Pan, M.; He, J. T.; Hng, H. H.; Yan, Q. Y.; Chen, H. Y. *J. Am. Chem. Soc.* **2010**, *132*, 9537.
7. Blanazs, A.; Armes, S. P.; Ryan, A. *J. Macromol. Rapid Commun.* **2009**, *30*, 267.
8. Cavalieri, F.; Hamassi, A. E.; Chiessi, E.; Paradossi, G. *Langmuir* **2005**, *21*, 8758.

9. Levine, D. P.; Ghoroghchian, P. P.; Freudenberg, J.; Zhang, G.; Therien, M. J.; Greene, M. I.; Hammer, D. A.; Murali, R. *Methods* **2008**, *46*, 25.
10. Jung, Y. K.; Kim, T. W.; Kim, J.; Kim, J. M.; Park, H. G. *Adv. Funct. Mater.* **2008**, *18*, 701.
11. Kolusheva, S.; Zadmard, R.; Schrader, T.; Jelinek, R. *J. Am. Chem. Soc.* **2006**, *128*, 13592.
12. Narayan, P.; Marchant, D.; Wheatley, M. A. *J. Biomed. Mater. Res.* **2001**, *56*, 333.
13. Schutt, E. G.; Klein, D. H.; Mattrey, R. M.; Riess, J. G. *Angew. Chem. Int. Ed.* **2003**, *42*, 3218.
14. Cheng, D.; Zhou, X.; Xia, H.; Xhan, H. S. O. *Chem. Mater.* **2005**, *17*, 3578.
15. Crespy, D.; Stark, M.; Hoffann-Richter, C.; Ziener, U.; Landfester, K. *Macromolecules* **2007**, *40*, 3122.
16. Broz, P.; Driamov, S.; Ziegler, J.; Ben-Haim, N.; Marsch, S.; Meier, W.; Hunziker, P. *Nano Lett.* **2006**, *6*, 2349.
17. Sanlés-Sobrido, M.; Pérez-Lorenzo, M.; Rodríguez-González, B.; Salgueiriño, V.; Correa-Duarte, M. A. *Angew. Chem. Int. Ed.* **2012**, *51*, 3877.
18. Cochran, J. K. *Solid State Mater. Sci.* **1998**, *3*, 474.
19. Häfeli, U.; Schütt, W.; Teller, J.; Zborowski, M. *Sci. Clin. Appl. Magn. Carriers* **1997**, *324*, 3791.
20. Sato, Y.; Takikawa, T.; Takishima, S.; Masuoka, H. *J. Supercrit. Fluids* **2001**, *19*, 187.
21. Di Maio, E.; Mensitieri, G.; Iannace, S.; Nicolais, L.; Li, W.; Flumerfelt, R. W. *Polym. Eng. Sci.* **2005**, *45*, 432.
22. Lee, J. W. S.; Park, C. B. *Macromol. Mater. Eng.* **2006**, *291*, 1233.
23. Champion, J. A.; Mitragotri, S. *Proc. Natl. Acad. Sci.* **2006**, *104*, 4930
24. Contaldi, V.; Pastore Carbone, M. G.; Di Maio, E.; Manikas, A. C.; Netti, P. A. *RCS Adv.* **2016**, *6*, 64140.
25. Im, S. H.; Jeong, U. Y.; Xia, Y. N. *Nat. Mater.* **2005**, *4*, 671.